Lipopolysaccharides Trigger Two Successive Bursts of Reactive Oxygen Species at Distinct Cellular Locations[1][OPEN]

Keke Shang-Guan,[a] Min Wang,[a] Nang Myint Phyu Sin Htwe,[a] Ping Li,[a] Yaoshen Li,[a] Fan Qi,[a] Dawei Zhang,[a] Min Cao,[a] Chanhong Kim,[b] Haiyong Weng,[c] Haiyan Cen,[c] Ian M. Black,[d] Parastoo Azadi,[d] Russell W. Carlson,[d] Gary Stacey,[e] and Yan Liang[a,2]

[a]College of Agriculture and Biotechnology, Zhejiang University, Hangzhou 310058, China
[b]Shanghai Center for Plant Stress Biology, Shanghai Institutes for Biological Sciences, Chinese Academy of Sciences, Shanghai 201602, China
[c]College of Biosystems Engineering and Food Science, Zhejiang University, Hangzhou 310058, China
[d]Complex Carbohydrate Research Center, University of Georgia, Athens, Georgia 30602
[e]Divisions of Plant Science and Biochemistry, Christopher S. Bond Life Sciences Center, University of Missouri, Columbia, Missouri 65211

ORCID IDs: 0000-0002-0948-7121 (K.S.-G.); 0000-0001-7075-7517 (I.M.B.); 0000-0001-5450-7235 (R.W.C.); 0000-0002-1248-8563 (Y.L.).

Lipopolysaccharides (LPS) are major components of the outer membrane of gram-negative bacteria and are an important microbe-associated molecular pattern (MAMP) that triggers immune responses in plants and animals. A previous genetic screen in Arabidopsis (*Arabidopsis thaliana*) identified LIPOOLIGOSACCHARIDE-SPECIFIC REDUCED ELICITATION (LORE), a B-type lectin *S*-domain receptor kinase, as a sensor of LPS. However, the LPS-activated LORE signaling pathway and associated immune responses remain largely unknown. In this study, we found that LPS trigger biphasic production of reactive oxygen species (ROS) in Arabidopsis. The first transient ROS burst was similar to that induced by another MAMP, flagellin, whereas the second long-lasting burst was induced only by LPS. The LPS-triggered second ROS burst was found to be conserved in a variety of plant species. Microscopic observation of the generation of ROS revealed that the LPS-triggered second ROS burst was largely associated with chloroplasts, and functional chloroplasts were indispensable for this response. The lipid A moiety, the most conserved portion of LPS, appears to be responsible for the second ROS burst. Surprisingly, the LPS- and lipid A-triggered second ROS burst was only partially dependent on LORE. Together, our findings provide insight on the LPS-triggered ROS production and the associated signaling pathway.

Plant innate immunity is initiated by the recognition of microbe-associated molecular patterns (MAMPs), leading to MAMP-triggered immunity (MTI). MAMPs are structural motifs that are highly conserved in microbes; for example, bacterial flagellin, elongation factor Tu, peptidoglycan, and fungal chitin (Nürnberger et al., 2004). Plants use membrane-associated pattern recognition receptors (PRRs) to sense MAMPs. Most PRRs belong to the Leu-rich repeat receptor-like kinases, lysin motif (LysM, the conserved 40-amino acid motif that recognizes GlcNAc oligomers) receptor-like proteins, and lectin receptor kinases (Boller and Felix, 2009; Antolín-Llovera et al., 2012; Choi et al., 2014; Liang et al., 2014; Macho and Zipfel, 2014; Ranf et al., 2015).

MTI includes a wide variety of responses, such as the elevation of cytosolic calcium ($[Ca^{2+}]_{cyt}$), production of reactive oxygen species (ROS), activation of mitogen-activated protein (MAP) kinases, expression of defense-related genes, deposition of callose, and restriction of pathogen growth (Jones and Dangl, 2006). The MAMP-triggered ROS burst is one of the best characterized MTI responses. The ROS burst is produced in the apoplast and is often very fast and transient, induced a few minutes after elicitor treatment, reaching a peak within 30 min, and subsequently dropping to basal levels within an hour (Baker and Orlandi, 1995; Lamb and Dixon, 1997). In Arabidopsis (*Arabidopsis thaliana*), the flagellin-triggered rapid ROS burst is mediated by plasma membrane-localized NADPH oxidase RBOHD (Respiratory Burst Oxidase Homolog D) and class III cell wall peroxidases (Torres et al., 2002; Daudi et al., 2012; O'Brien et al., 2012; Kadota et al., 2014; Li et al., 2014). However, some elicitors were found to trigger a more complicated ROS burst. AsES (Elicitor and Subtilisin), an elicitor from *Acremonium strictum*, causes a triphasic ROS burst in strawberry (*Fragaria* spp.) suspension cells, with peaks at 30 min, 2 h, and 7 h after treatment (Martos et al., 2015). INF1 (INFESTANS1), a major elicitor secreted by *Phytophthora infestans*, triggers a late ROS burst in *Nicotiana benthamiana*, which is mediated by transcriptional activation of *RBOHB*, an *AtRBOHD* ortholog, via the MAPK-WRKY pathway (Adachi et al., 2015).

Lipopolysaccharides (LPSs; also referred to as endotoxin) are abundant in the outer cell envelope of gram-negative bacteria and are indispensable for bacterial viability and survival. In mammals, bacterial LPS act as a strong MAMP that is sensed by the membrane-associated Toll-like receptor 4 (TLR4), leading to activation of a variety of innate immune responses, including ROS production (Lambeth, 2004; Lu et al., 2008; Song and Lee, 2012; Storek and Monack, 2015). Although LPS-induced ROS production is believed to be mediated by NADPH oxidases, mitochondrial ROS production has been implicated in LPS-induced proinflammatory responses (West et al., 2011; Sena and Chandel, 2012; Park et al., 2015; Pinegin et al., 2018). Recently, other TLR4-independent intracellular receptors, namely human caspase 4/5 and mouse caspase 11, were reported to play a role in LPS-triggered noncanonical inflammasome activation (Hagar et al., 2013; Mahla et al., 2013; Yang et al., 2015). However, whether this intracellular LPS recognition can induce ROS production is still unclear.

In plants, LPS are also considered MAMPs, but plant responses can be quite variable depending on the plant species examined and the microbial source of LPS. For example, LPS from the plant pathogen *Xanthomonas capestris* were shown to induce an ROS burst in cultured cells of tobacco (*Nicotiana tabacum*; Braun et al., 2005), whereas LPS from *Pseudomonas syringae* did not induce an ROS burst in tobacco leaves (Ranf et al., 2015). In Arabidopsis cells, different kinetics of the ROS burst were observed using LPS derived from pathogenic and nonpathogenic bacteria, and ROS were detected in the cytosol (Mohamed et al., 2015). These variable immune responses present a challenge regarding identification of the common plant components involved in LPS recognition and the related signal transduction events. This may explain why a plant receptor for LPS was only recently identified (Ranf et al., 2015). Ranf and colleagues found that LPS from *Pseudomonas* and *Xanthomonas* triggered a rapid elevation of $[Ca^{2+}]_{cyt}$ in Arabidopsis, and subsequently isolated an LPS-insensitive mutant *lore* (*lipooligosaccharide-specific reduced elicitation*; Ranf et al., 2015). *LORE* encodes the SD1-29 protein (B-type lectin *S*-domain receptor kinase). Phylogenetic analysis has indicated that LORE is restricted to the family Brassicaceae, suggesting that LORE-mediated immunity is not a general LPS response in the plant kingdom (Ranf et al., 2015). Recently, it was reported that the chitin receptor CERK1 (Chitin Elicitor Receptor Kinase 1) might play a role in LPS recognition in rice (*Oryza sativa*), but not in Arabidopsis (Desaki et al., 2018). Overall, LPS-induced innate immune responses, as well as the associated signal transduction cascades, are largely uncharacterized.

In this study, we compared LPS-triggered immune responses with the well-characterized MAMP, flg22 (a conserved peptide of bacterial flagellin). Compared with flg22, LPS-triggered early MTI responses were weaker, whereas the late MTI responses were as strong as or even stronger than those induced by flg22. Hence, this aroused our interest in studying the phenomenon in greater detail. We found that LPS induced a long-lasting second burst of ROS, which appears to be conserved based on tests conducted using other dicot and monocot plants. Unlike the flg22-induced rapid apoplastic ROS burst, LPS triggered a second ROS burst that appeared to be largely centered in the chloroplast. The lipid A moiety appears to be mainly responsible for this intracellular ROS burst. These LPS- and lipid A-triggered second ROS bursts were present in *lore* mutants, albeit at significantly reduced levels. Taken together, our results indicate the existence of multiple pathways in which LPS are sensed as a MAMP.

RESULTS

LPS Trigger Weak Early but Strong Late MTI Responses

To investigate LPS-triggered innate immune responses, we compared typical MTI responses induced by LPS and flg22. Previously, it was shown that 10 to 50 μg/mL commercial LPS purified from *Pseudomonas aeruginosa* can trigger plant innate immune responses (Sun et al., 2012; Ranf et al., 2015). Therefore, in our initial experiments, we used 50 μg/mL LPS, whereas 100 nM flg22, a moderate concentration (Gómez-Gómez and Boller, 2000; Zipfel et al., 2004), was used as a control. Flg22 triggered typical early MTI responses within 30 min, including elevation of $[Ca^{2+}]_{cyt}$, an ROS

[1] This work was supported by the National Natural Science Foundation of China (31622006 to Y.L.; 31600988 to K.S.-G.), the Fundamental Research Funds for the Central Universities (to Y.L.), and the China Postdoctoral Science Foundation (2016M590543 to K.S.-G.). Additional support came from the National Institute of General Medical Sciences of the National Institutes of Health under award no. R01GM121445 (to G.S.). The content of this article is solely the responsibility of the authors and does not necessarily represent the official views of the National Institutes of Health. This work was also supported by the Next-Generation BioGreen 21 Program Systems and Synthetic Agrobiotech Center, Rural Development Administration, Republic of Korea (PJ01116604 to G.S.) and by the Chemical Sciences, Geosciences and Biosciences Division, Office of Basic Energy Sciences, U.S. Department of Energy (grant DE-SC0015662 to P.A.) at the Complex Carbohydrate Research Center.

[2] Address correspondence to yanliang@zju.edu.cn.

The author responsible for distribution of materials integral to the findings presented in this article in accordance with the policy described in the Instructions for Authors (www.plantphysiol.org) is: Yan Liang (yanliang@zju.edu.cn).

Y.L. and G.S. planned and designed the research; K.S.-G. and M.W. performed most of the experiments; N.M.P.S.H. contributed to the confocal observation of ROS; M.C. contributed to the $[Ca^{2+}]_{cyt}$ analysis; D.Z., F.Q., and Y.S.L. contributed to the ROS assay for mutants; C.K. contributed to SSU-GFP observations; H.W. and H.C. contributed to the photosynthesis assay; P.L., I.M.B., P.A., and R.W.C. contributed to LPS and lipid A isolation; G.S. and Y.L. wrote the manuscript.

[OPEN] Articles can be viewed without a subscription.

www.plantphysiol.org/cgi/doi/10.1104/pp.17.01637

burst, MAP kinase activation, and induction of defense-related gene expression. Although LPS induced a rapid elevation of $[Ca^{2+}]_{cyt}$ in the transgenic seedlings carrying the calcium reporter aequorin, consistent with previously published results (Ranf et al., 2015), this response was significantly weaker than that seen with flg22 (Fig. 1A). A rapid ROS burst was observed after LPS treatment, but this was considerably lower than that seen upon flg22 treatment (Fig. 1B). It is worth noting that LPS itself inhibits luminol activity in vitro (Supplemental Fig. S1), and therefore the actual ROS level triggered by LPS might be higher than what can be measured. Similarly, MAP kinase activation after LPS treatment was barely detectable by immunoblotting with an antiphospho-p42/p44 MAP kinase antibody. A response could only be detected when larger

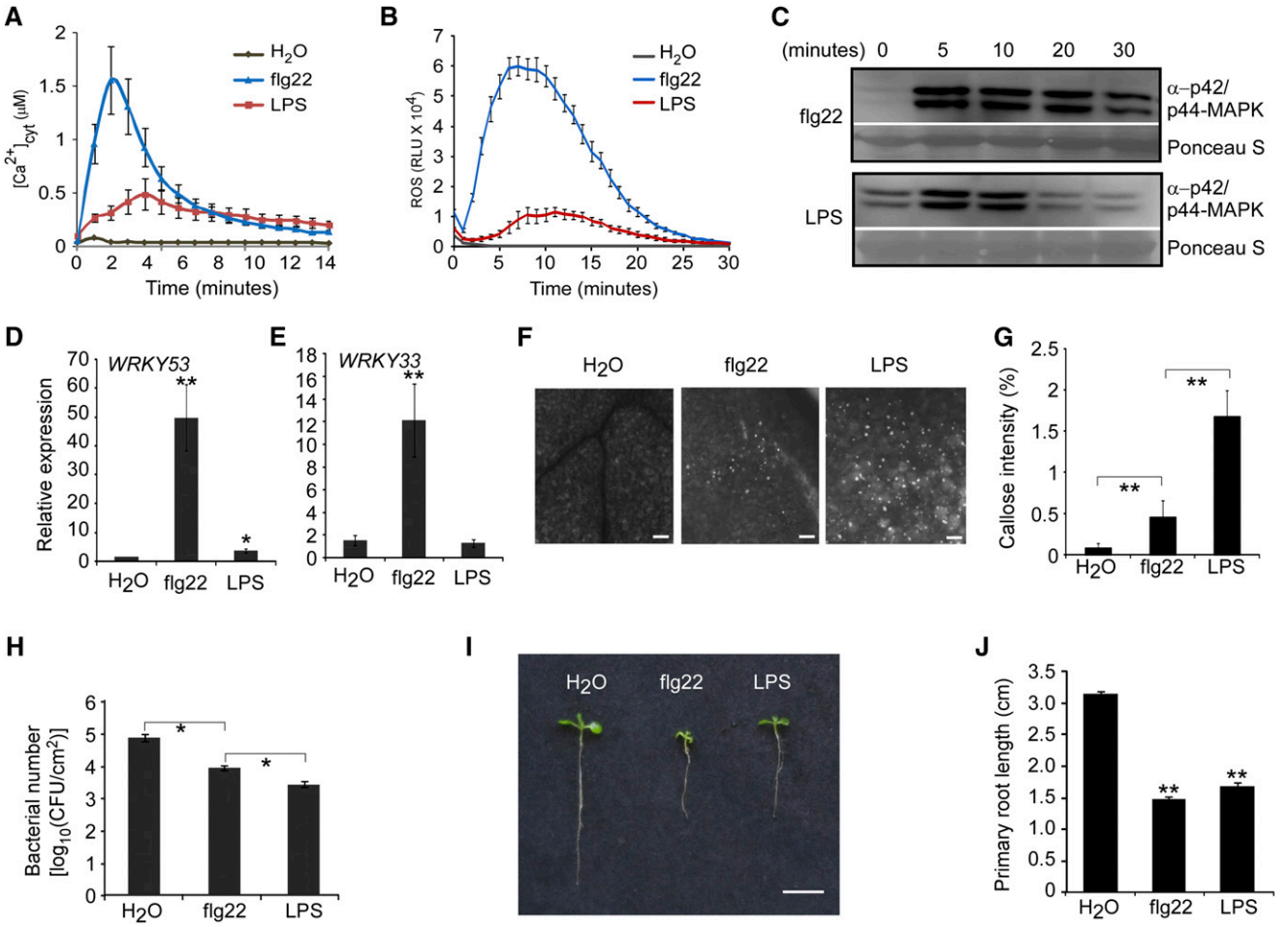

Figure 1. LPS trigger weak early, but strong late MAMP-triggered immunity responses. A, Elevation of $[Ca^{2+}]_{cyt}$. $[Ca^{2+}]_{cyt}$ was measured using 5-d-old transgenic seedlings expressing the calcium reporter protein, aequorin. Signals were recorded for 15 min after treatment. B, ROS burst. ROS were monitored using a chemiluminescence assay with luminol as a substrate. Leaf disks were punched from 4-week-old mature plants. Signals were recorded for 30 min after treatment. C, MAP kinase phosphorylation. Total protein was extracted from 10-d-old seedlings at different time points after treatment. Immunoblot analysis was performed using an antip42/p44-MAPK antibody. Ponceau S staining was used for protein loading control. D and E, *WRKY53* (D) and *WRKY33* (E) gene expression. Gene expression was quantified by RT-qPCR. RNA was extracted from 10-d-old seedlings 30 min after treatment. *UBQ10* was used as the reference gene. F, Callose deposition. Ten-day-old seedlings were treated with water, flg22, or LPS for 24 h. Callose was stained with aniline blue. Representative images are shown. Bars = 100 μm. G, Quantification of the callose intensity in F. The percentages were quantified as the number of fluorescent callose-corresponding pixels relative to the total number of pixels covering the cotyledon surface using Image J software. H, Growth of *P. syringae* pv. *tomato* DC3000 (*Pst* DC3000). Five-week-old Arabidopsis leaves were primed with the indicated treatment before bacterial infection. The inoculation concentration of *Pst* DC3000 was 10^5 cfu/mL. Bacterial growth was determined 3 d after inoculation. I, Inhibition of seedling growth. Five-day-old seedlings were transferred to the indicated liquid media and images were taken 5 d after incubation. Bar = 1 cm. J, Primary root length in I. LPS (50 μg/mL) and flg22 (100 nM) were used in these assays. The data are shown as means ± SE ($n = 8$ in A, B, G, and J; $n = 3$ in D, E, and H). Asterisks indicate significant differences from the control treatment (Student's paired *t* test: $*P \leq 0.05$, $**P \leq 0.01$). All experiments were repeated twice with similar results.

amounts of protein were loaded and when using a long exposure time to develop the membrane (Fig. 1C). In addition, we examined transcriptional induction of the defense-responsive genes *WRKY33* and *WRKY53* 30 min after LPS or flg22 treatment. Only *WRKY53* showed a slight induction after LPS treatment, whereas both genes were highly induced by flg22 (Fig. 1, D and E). Collectively, these results indicate that LPS-triggered early MTI responses are considerably weaker compared with those triggered by flg22.

We next compared some typical late MTI responses to LPS and flg22 treatment. Callose deposition was detected by aniline blue staining 24 h after LPS or flg22 treatment. We found that the intensity of LPS-triggered callose was significantly higher than that triggered by flg22 (Fig. 1, F and G). Pretreatment with flg22 or LPS restricted *P. syringae* growth, whereas in contrast to other measures (e.g. $[Ca^{2+}]_{cyt}$), LPS showed stronger restriction than flg22 (Fig. 1H). Seedling growth inhibition is another long-term response to flg22 elicitation, and therefore primary root length was measured 5 d after seedlings had been transferred to medium containing flg22 or LPS. LPS showed similar inhibition of primary root length, as seen with flg22 (Fig. 1, I and J). Therefore, unlike the early responses, LPS-triggered late responses appeared stronger than or equal to those induced by flg22. These data indicate that LPS may induce a signaling pathway that differs from that induced by flg22, leading to stronger late responses.

LPS Induce a Strong Second ROS Burst

To explore possible alternative signaling pathways for LPS, we monitored all early responses from 1 h to 24 h after treatment. Interestingly, we found that LPS induced a biphasic elevation of ROS, whereas treatment with flg22 showed only a single, rapidly appearing peak relative to the water control (Supplemental Fig. S2). The second long-lasting LPS-induced ROS burst commenced after 2 h, reached a peak after ~3 to 10 h, and then decreased to basal levels after ~20 h (Fig. 2A). Occasionally, two peaks and a longer duration were observed (Supplemental Fig. S2). Moreover, when observed, the earlier response was invariably significantly weaker than the later response. To focus attention on the later LPS responses, a graph was plotted from 1 h to 24 h after elicitor treatment, which avoids the very large peak that occurs prior to 1 h due to the ROS triggered by flg22 (Fig. 2A). The kinetics and magnitude of the second ROS burst were dose dependent, and could be induced by LPS concentrations greater than 10 μg/mL (Fig. 2B). Overall, although LPS were found to induce a second ROS burst, it did not induce MAP kinase activation (Supplemental Fig. S3). However, we cannot rule out the possibility that the sampling times we used may have missed a narrow window of MAP kinase activation. We also examined *WRKY* gene expression at 1, 3, 5, 10, and 24 h after LPS or flg22 treatment. The transcripts of *WRKY33* and *WRKY53* were significantly induced from 3 h to 24 h after LPS treatment, corresponding to the timing of the second ROS burst (Fig. 2, C and D). The transcripts of *OXI1* (*OXIDATIVE SIGNAL-INDUCIBLE1*), a gene regulated by ROS, also reflect similar kinetics (Fig. 2E). Together, these results indicate that LPS trigger a second ROS signaling pathway that reprograms certain defense-responsive genes, which we assume explains the strong late responses.

As noted above, the presence of the LORE receptor appears to be specific to the Brassicaceae (Ranf et al., 2015). Therefore, it was of interest to determine whether plant species outside Brassicaceae also showed the LPS-triggered second ROS burst. Although not an exhaustive list, all the plants we examined (three other dicot species: tomato [*Lycopersicum esculentum*], *Nicotiana benthamiana*, and soybean [*Glycine max*], and two monocot species: rice and barley [*Hordeum vulgare*]) exhibited a late ROS response upon LPS elicitation. Not all these plants showed a ROS burst within 1 h, but all showed a late ROS burst with a peak occurring ~1 to 10 h after LPS treatment (Supplemental Fig. S4). The absolute ROS levels in the monocot species were lower than those measured in the dicot plants (Fig. 2, F and G). Together, these results indicate that the LPS-triggered second ROS burst is probably conserved within a wide range of plant species. Given that LORE is specific to the Brassicaceae, it is most likely that, in species from other families, another receptor(s) is involved in the LPS-triggered second ROS burst.

LPS Trigger Intracellular ROS Production

In plants, ROS production induced by activation of plasma membrane-associated MAMP receptors is largely localized to the apoplast (Mignolet-Spruyt et al., 2016). However, in some situations, ROS can be produced in intracellular compartments, including chloroplasts, peroxisomes, and mitochondria (Camejo et al., 2016; Mignolet-Spruyt et al., 2016). To localize the LPS-triggered second ROS burst, we used isoluminol, which is a luminol homolog that is cell membrane impermeable and therefore can be used only to measure apoplastic ROS production. By contrast, luminol can be used to measure both extracellular and intracellular ROS. Given that the flg22-triggered rapid ROS burst has been confirmed to occur in the apoplast, this served as a good control for our experiments. We adjusted the isoluminol concentration relative to luminol to achieve a similar magnitude of flg22-triggered apoplast ROS burst (Supplemental Fig. S5). Compared with luminol, no strong second ROS burst could be detected after LPS treatment when isoluminol was used as a substrate for the chemiluminescence assay (Fig. 3A), indicating that the second ROS burst triggered by LPS occurs at an intracellular location.

To examine which cellular compartment might be responsible for the LPS-triggered second ROS burst, we performed 3,3-diaminobenzidine (DAB) staining 8 h after flg22 or LPS treatment. DAB precipitates in the presence of hydrogen peroxide (H_2O_2), and therefore

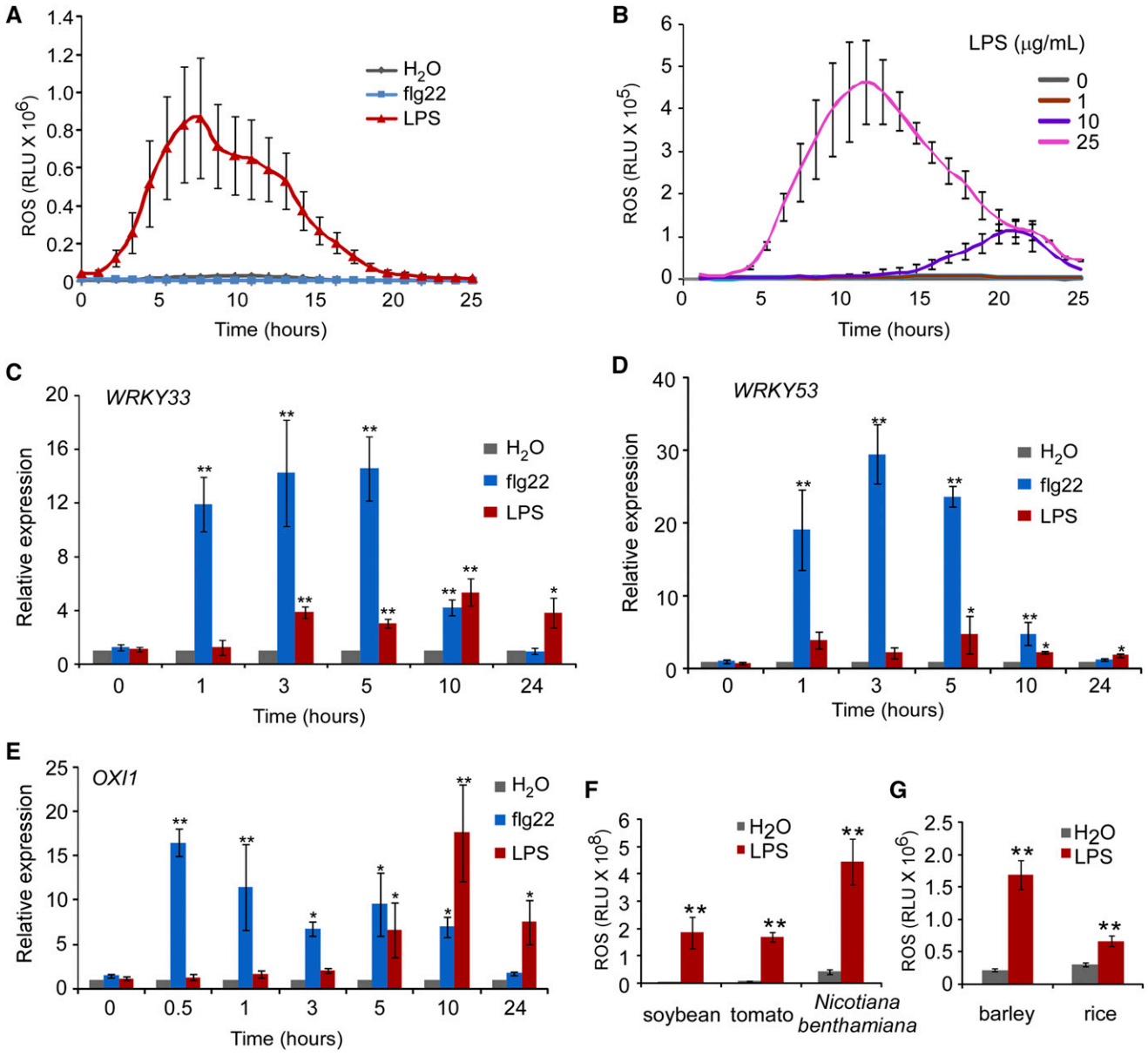

Figure 2. LPS trigger an ROS burst. A and B, LPS-induced second ROS burst. ROS production was monitored using a chemiluminescence assay with luminol as a substrate. Leaf disks were punched from 4-week-old mature plants. LPS (50 μg/mL) and flg22 (100 nM) were used in A. The LPS concentration in B is indicated in the figure. Signals were recorded for 24 h after treatment. The data are shown as means ± SE ($n = 8$). C to E, *WRKY33* (C), *WRKY53* (D), and *OXI1* (E) gene expression. Gene expression was quantified by RT-qPCR. RNA was extracted from 10-d-old seedlings at the indicated time points after treatment. *UBQ10* was used as the reference gene. The data are shown as means ± SE from three biological replicates. Asterisks indicate significant differences from the value at the 0 h time point (Student's paired *t* test: $*P \leq 0.05$, $**P \leq 0.01$). F and G, ROS burst in representative dicot (F) and monocot (G) species after LPS treatment. The bar graph indicates the total integrated photon counts within 24 h after treatment. The data are shown as means ± SE ($n = 8$). Asterisks indicate significant differences between LPS and control treatments (Student's paired *t* test: $*P \leq 0.05$, $**P \leq 0.01$). LPS (50 μg/mL) and flg22 (100 nM) were used in these assays. All experiments were repeated twice with similar results.

should localize at the site(s) where H_2O_2 is generated. Compared with flg22, stronger DAB staining, as indicated by a brown color, was observed after LPS treatment (Fig. 3B), and the staining was largely associated with chloroplasts (Fig. 3C). In addition, we performed dichlorodihydrofluorescein (DCF) staining to directly visualize the subcellular compartments in which the LPS-induced ROS burst occurs. This fluorogenic dye

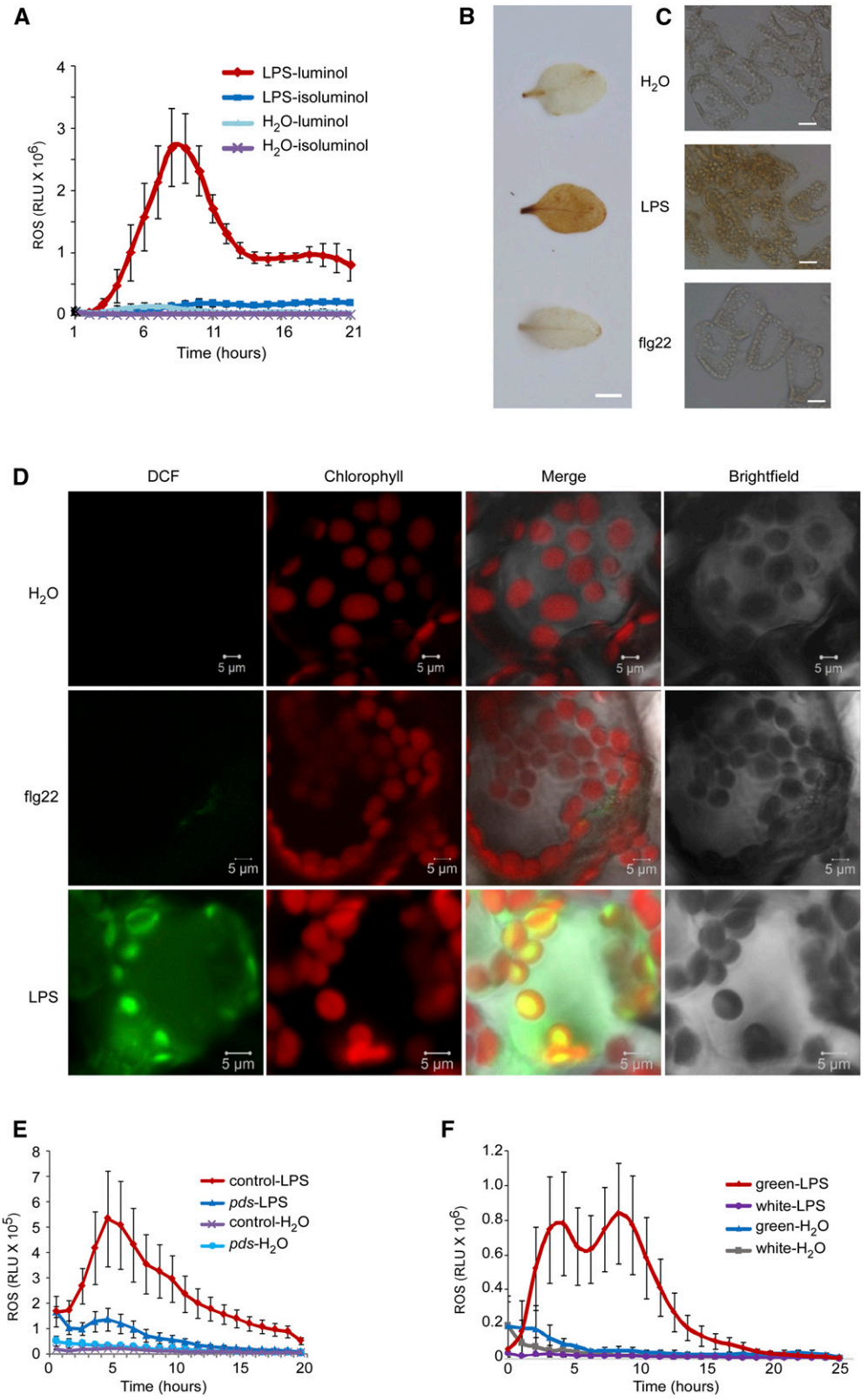

Figure 3. The LPS-triggered second ROS burst is associated with chloroplasts. A, ROS burst. ROS were monitored using a chemiluminescence assay with either luminol or isoluminol as a substrate. Leaf disks were punched from 4-week-old mature plants. Signals were recorded for 21 h after LPS (50 μg/mL) or water treatment. B and C, Accumulation of H_2O_2 in 4-week-old leaves. H_2O_2 generation was detected by DAB staining 8 h after water, LPS (50 μg/mL), or flg22 (100 nM) treatment. The brown color indicates strong H_2O_2 production. DAB-stained leaves in B were examined under a microscope (C). Bars = 5 mm (B) and 20 μm (C). D, Fluorescence detection of intracellular ROS. Two-week-old seedlings were treated with water, LPS (50 μg/mL), or flg22 (100 nM) for 1 h. ROS were detected by CM-H2DCFDA staining. ROS fluorescence (green) and chlorophyll autofluorescence (red) were analyzed under a confocal microscope. Bars = 10 μm. E, ROS burst in *PDS*-silenced leaves. *PDS* was silenced in tomato leaves using the virus-induced gene silencing (VIGS) approach. The empty vector was used as a negative control. Leaf disks were punched 20 d after VIGS. ROS production was monitored for 20 h after LPS (50 μg/mL) or water treatment using a chemiluminescence assay with luminol as a substrate. F, ROS burst in Arabidopsis *var2* mutants. Leaf disks from white sectors and green sectors of *var2* mutants were used for measurement of ROS. ROS were monitored for 24 h after LPS (50 μg/mL) or water treatment using a chemiluminescence assay with luminol as a substrate. The data (A, E, and F) are shown as means ± SE (n = 8). All experiments were repeated twice with similar results.

can diffuse through the plasma membrane into the cell where it is deacetylated by intracellular esterases (Jakubowski and Bartosz, 2000). Subsequent oxidation by ROS produces a highly fluorescent compound within the cell. LPS clearly induced strong green fluorescence inside the cell, and this was largely colocalized

with chlorophyll autofluorescence (red color) in both mesophyll and stomatal cells (Fig. 3D; Supplemental Fig. S6A). These data strongly suggest that the LPS-induced second ROS burst is largely associated with chloroplasts. However, given that the production of chloroplastic, mitochondrial, and peroxisomal ROS is tightly interconnected (Mignolet-Spruyt et al., 2016), it is difficult to state unequivocally that the chloroplast is the sole source of the intracellular ROS. Notably, when young seedlings were used in this assay, which allowed better penetration of the fluorogenic dye, ROS could be detected 1 h after LPS treatment, which was considerably earlier than the ROS burst detected by DAB staining in mature leaves. This observation indicates that young seedlings might be more sensitive to LPS. Repeating the DAB staining with young seedlings showed the presence of a strong brown color within 1 h after LPS treatment (Supplemental Fig. S6B). Therefore, all three assays with DAB and fluorogenic dye staining consistently indicated that the LPS-triggered second ROS burst is mainly associated with chloroplasts.

If chloroplasts are the major sites at which ROS are generated after LPS treatment, we assumed that functional chloroplasts would be required for this response. To test this hypothesis, we used either the Arabidopsis leaf-variegated *variegated2* (*var2*) mutant line or tomato plants in which *PHYTOENE DESATURASE* (*PDS*) had been silenced. Loss of *PDS* results in loss of pigment, as is also the case in the white sectors of *var2* mutants. The LPS-triggered second ROS burst could not be detected in leaves with little or no pigment (Fig. 3, E and F), whereas these mutants showed a normal response to flg22 elicitation (Supplemental Fig. S7, A and B). During darkness, chlorophyll is degraded (Hörtensteiner, 2006). Accordingly, we observed that when leaf disks were incubated under dark conditions overnight, the LPS-triggered second ROS burst was diminished (Supplemental Fig. S7, C and D). Therefore, differentiated functional chloroplasts appear to be indispensable for the LPS-triggered second ROS burst.

LPS Impair Chloroplast Development and Function

We next examined whether LPS could impair chloroplast development and function. Effects on chloroplast development were detected in transgenic plants expressing the nuclear-encoded and chloroplast-localized small subunit of ribulose-1.5-bisphosphate carboxylase (SSU) fused to the GFP. GFP was detected by confocal microscopy 3 h after the MAMP treatment. Following either water or flg22 treatment, the GFP signal overlapped with chlorophyll autofluorescence, whereas GFP appeared to be released from chloroplasts upon LPS treatment, an effect similar to that seen upon addition of the herbicide paraquat, which inhibits photosynthesis (Fig. 4A).

These observations led us to directly examine the effect of LPS on photosynthetic capacity by monitoring chlorophyll fluorescence in 2-week-old seedlings with or without LPS treatment. The photosynthetic efficiency of PSII in a dark-adapted state (F_v/F_m) was significantly reduced 2 h after LPS treatment (Fig. 4B). In addition, we found that nonphotochemical quenching (NPQ; a photoprotective process that converts excess excitation energy into heat) increased transiently 2 to 6 h after LPS treatment (Fig. 4C). These results suggest a profound effect of LPS on chloroplast development and photosynthetic capacity.

The Lipid A Moiety Appears to Be Largely Responsible for the Intracellular ROS Burst

In most bacteria, LPS consist of three regions, an *O*-specific repetitive oligosaccharide chain (termed the *O*-antigen), a covalently linked nonrepetitive core oligosaccharide region (termed the core oligosaccharide), and a hydrophobic lipid region (termed lipid A; King et al., 2009; Lam et al., 2011). The lipid A moiety of LPS confers endotoxic activity and is responsible for both TLR4- and caspase-mediated immune responses in mammals, as well as LORE-mediated responses in Arabidopsis (Lu et al., 2008; Song and Lee, 2012; Ranf et al., 2015; Storek and Monack, 2015). To examine whether the lipid A moiety is required for the intracellular ROS burst, we extracted LPS from *P. aeruginosa* PAO1 and *P. syringae* pv. *tomato* DC3000. The ROS burst induced by the lipid A isolated from both strains was compared with that induced by LPS. The purity of LPS and lipid A was examined by running SDS-PAGE gels (Supplemental Fig. S8). For comparison with 25 μg/mL lipid A, a concentration used for the detection of early ROS burst (Ranf et al., 2015), we used 25 μg/mL LPS in this experiment. Similar to the commercial LPS, the LPS extracted from PAO1 and DC3000 induced weak early, but strong late ROS production (Fig. 5). The purified lipid A triggered a relatively stronger early ROS response compared with LPS; however, this was still weaker than the response induced by flg22 (Supplemental Fig. S9). Each of the purified lipid A preparations triggered a second long-lasting ROS burst (Fig. 5). Collectively, these results indicate that the lipid A moiety is responsible for the intracellular ROS burst.

The LPS-Triggered Intracellular ROS Burst Is Reduced but Still Present in *lore* Mutant Plants

In Arabidopsis, LPS are sensed by LORE, and *lore* mutants (*sd1-29*, T-DNA insertion mutants of *LORE*) are defective in the rapid LPS-induced ROS burst (Ranf et al., 2015; Fig. 6A). However, this initial report did not examine the later second LPS-induced ROS burst. Therefore, we measured this response in wild-type and *lore* mutant plants and, to our surprise, found that the second ROS burst was still present in the *lore* mutants after treatment with 50 μg/mL LPS, albeit delayed compared with the wild-type response (Fig. 6B). We also examined the second ROS burst using 25 μg/mL LPS and found that the *lore* mutants still showed responses, mimicking the ROS kinetics observed in the

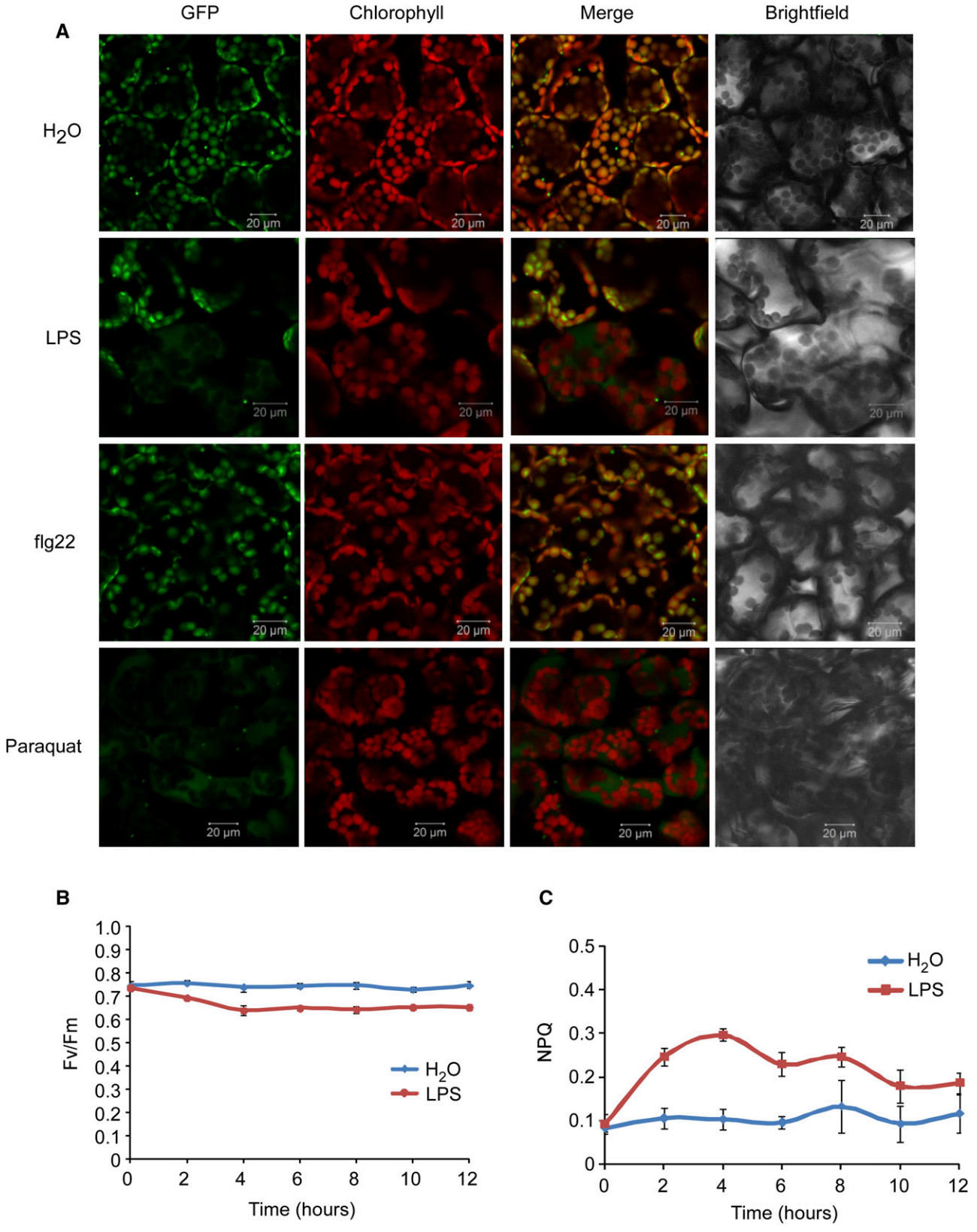

Figure 4. LPS impair chloroplast development and function. A, LPS impair chloroplast development. Transgenic plants expressing the SSU fused to the GFP were treated with water, flg22 (100 nM), or LPS (50 μg/mL) for 3 h. GFP and chlorophyll autofluorescence were detected under a confocal microscope. Paraquat (1 μM) was used as the positive control for the release of

wild-type plants in response to treatment with 10 μg/mL LPS (Figs. 6C and 2B). These results indicate that the LPS-triggered second ROS burst is not diminished in *lore* mutants. Similarly, compared with wild-type plants, the lipid A-triggered second ROS burst was reduced in *lore* mutant plants but still present (Fig. 6D).

To extend our observations, we also examined seedling growth inhibition after LPS and lipid A treatment (Fig. 6, E and F). Consistent with the second ROS effect, *lore* mutants still responded to LPS and lipid A, as demonstrated by the significant inhibition of seedling growth. In contrast to the *lore* mutants, the LPS-triggered second ROS burst was similar to that observed in the wild type when examined in loss-of-function mutants of known PRRs, including *FLAGELLIN SENSING2* (*FLS2*) and *BRASSINOSTEROID INSENSITIVE1-ASSOCIATED RECEPTOR KINASE1* (*BAK1*) for flagellin sensing, and *CERK1* and *LysM RECEPTOR KINASE5* (*LYK5*) for chitin sensing (Supplemental Fig. S10). Taken together, these observations reveal that although the LPS-triggered intracellular ROS burst is reduced in the *lore* mutant plants, it is still present, indicating the existence of a redundant LPS recognition step that functions largely to trigger the late responses to elicitor addition.

DISCUSSION

ROS are by-products of normal metabolism and also act as signaling molecules during development and stress responses (Galvez-Valdivieso and Mullineaux, 2010; Shapiguzov et al., 2012; Mignolet-Spruyt et al., 2016; Qi et al., 2017). Chloroplasts are the major sites for ROS production in plants, and chloroplastic ROS have been implicated as intermediates in retrograde signaling from chloroplasts to the nucleus (Asada, 2006; Maruta et al., 2012). In this study, we found that LPS triggered a substantially weaker early ROS burst and little or no detectable early MAPK phosphorylation changes, but also induced a second persistent elevation of ROS in the ensuing 4 to 24 h. The downstream gene expression corresponded to the timing of the second ROS burst after LPS treatment. Our results indicate that the LPS-induced second ROS burst acts as a signal that appears to induce a long-term response as strongly as or even stronger than flg22.

A biphasic accumulation of ROS has previously been reported to occur in plants after biotrophic pathogen attack (Baker and Orlandi, 1995; Lamb and Dixon, 1997). The first ROS burst generally reflects MAMP-triggered ROS production and is primarily localized to the apoplast. In Arabidopsis, a flagellin-triggered rapid ROS burst is mediated by plasma membrane-localized NADPH oxidases (Torres et al., 2002; Kadota et al., 2014; Li et al., 2014). The second ROS burst observed upon pathogen inoculation is associated with effector-triggered immune responses, which typically accompany the hypersensitive response (Liu et al., 2007; Zurbriggen et al., 2009). However, chloroplast-localized ROS production has been observed when Arabidopsis leaves are infected with a *hrpA* (*HR* and pathogenicity A) mutant of *P. syringae* pv. *tomato* DC3000, a strain that is defective in the type III secretion system, thereby indicating that some MAMPs can trigger a chloroplast ROS burst (de Torres Zabala et al., 2015). However, to our knowledge, the specific MAMP(s) that trigger this chloroplastic ROS burst have not been identified. In this study, we found that LPS, an important MAMP, could trigger an intracellular ROS burst that is probably generated in the chloroplasts. Although the LORE-mediated apoplastic rapid ROS burst appears specific to the Brassicaceae family of plants, this second long-lasting ROS burst in response to LPS was observed in a variety of dicots and monocots. Therefore, the LPS-triggered intracellular ROS burst may represent the major immune response to LPS in the plant kingdom and an initial event in MTI responses, which could be a useful model for deciphering the molecular mechanism of intracellular ROS burst.

Consistent with the observation that LORE is restricted to the Brassicaceae (Ranf et al., 2015), no LORE-mediated early ROS burst could be detected in *Nicotiana benthamiana*, tomato, barley, or rice. Interestingly, a strong early ROS burst could be induced in soybean after LPS treatment. In contrast, the LPS-triggered second ROS burst was observed in all these plant species. These data indicate the presence of an LPS recognition system, in addition to LORE, which is widely distributed in plants and mediates this second cytoplasmically localized ROS response to LPS elicitation. This hypothesis is consistent with our finding that the LPS-induced second ROS burst was still detectable in Arabidopsis *lore* mutants. These data indicate that in some cruciferous plants, like Arabidopsis, LORE-mediated recognition could potentiate a presumably more broadly conserved signaling pathway that involves a strong chloroplast-based ROS burst. At a minimum, the fact that *lore* mutant plants retain the intracellular response to LPS suggests that Arabidopsis has an alternative mechanism whereby it recognizes and responds to LPS, which is partially redundant to the LORE-mediated pathway.

Figure 4. (*Continued.*)
SSU-GFP from chloroplasts. Six seedlings were examined for each treatment. Bars = 20 μm. B, The photosynthetic efficiency of PSII in F_v/F_m. Two-week-old seedlings grown on half-strength MS agar in 6-well plates were treated with water or LPS (50 μg/mL), and chlorophyll fluorescence imaging was performed at the indicated time points after treatment. C, NPQ. Experimental conditions were the same as in B. The data are shown as means ± SE from three biological replicates. The experiment was repeated twice with similar results.

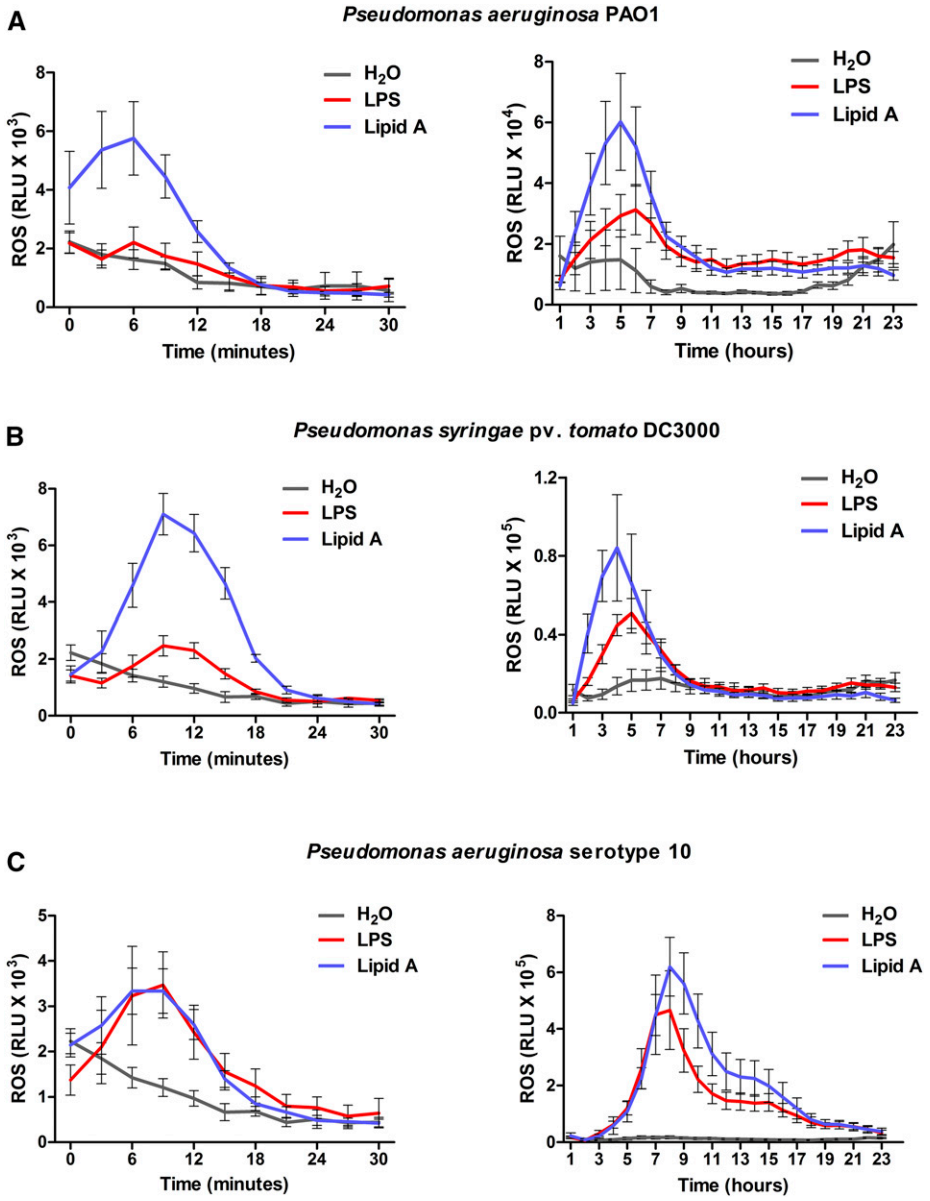

Figure 5. Lipid A is responsible for the second burst of ROS. A, The ROS burst triggered by lipid A and LPS extracted from *P. aeruginosa* PAO1. B, The ROS burst triggered by lipid A and LPS extracted from *P. syringae* pv. *tomato* DC3000. C, The ROS burst triggered by lipid A extracted from commercial LPS of *P. aeruginosa* serotype 10. LPS (25 μg/mL) and lipid A (25 μg/mL) were used in these assays. ROS was monitored for 24 h with luminol as a substrate. The data are shown as means ± SE (n = 8).

Although we found that lipid A is largely responsible for the intracellular ROS burst, we cannot rule out the possibility that core oligosaccharides also play a role. Previous studies reported that both the core oligosaccharide and lipid A from *X. campestris* can induce *PR1* and *PR2* expression in Arabidopsis, which is indicative of an immune response (Silipo et al., 2005). Core oligosaccharides were shown to induce an early but relatively weak up-regulation of gene expression at ~12 h after treatment, whereas lipid A triggered a substantially stronger gene expression ~20 h after treatment (Silipo et al., 2005).

Clearly, the details of the events leading to this second ROS burst induced by LPS remain to be elucidated. However, this work suggests that, in addition to LPS recognition by LORE in Arabidopsis, plants have probably evolved other pathways for LPS recognition and/or response. One exciting possibility that remains to be examined is that the intracellular responses to LPS in plant and mammalian cells may reflect conserved pathways, thereby providing evidence of a common need to recognize pathogens via LPS, a universal bacterial MAMP.

CONCLUSION

In conclusion, we found that LPS, an important MAMP, triggered two successive ROS bursts at distinct cellular locations in Arabidopsis. ROS play important

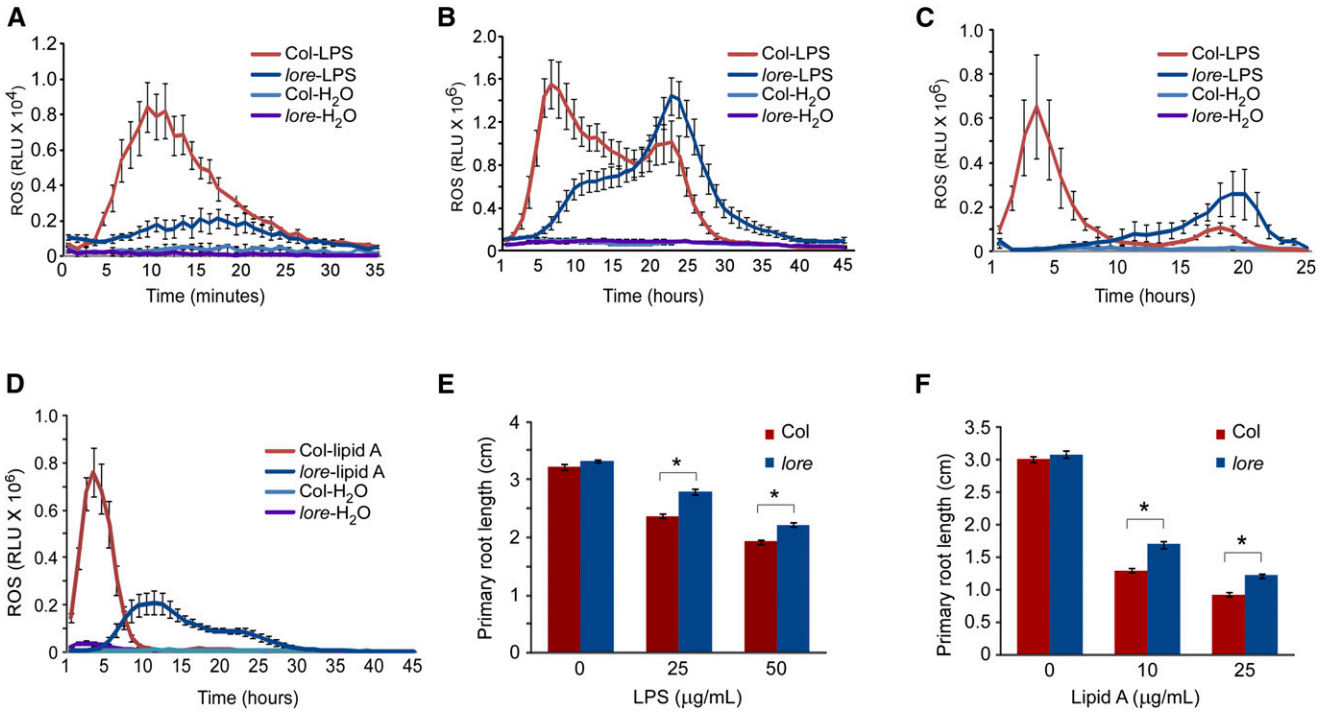

Figure 6. The LPS-triggered second ROS burst is only partially dependent on LORE. A, The first rapid ROS burst after treatment with 50 μg/mL LPS in wild-type and *lore* mutant plants. ROS were monitored for 30 min with 400 μM luminol as a substrate. B, The second ROS burst after treatment with 50 μg/mL LPS in wild-type and *lore* mutant plants. ROS were monitored for 45 h with 200 μM luminol as a substrate. C, The second ROS burst after treatment with 25 μg/mL LPS in wild-type and *lore* mutant plants. ROS were monitored for 25 h with 200 μM luminol as a substrate. D, The second ROS burst after treatment with 25 μg/mL lipid A in wild-type and *lore* mutants. ROS were monitored for 45 h with 200 μM luminol as a substrate. E and F, Inhibition of primary root length in wild-type and *lore* mutant plants. Five-day-old seedlings were transferred to the indicated liquid media and the primary root length was measured 5 d after incubation. The data are shown as means $\pm$ SE ($n = 18$). Asterisks indicate significant differences (Student's paired *t* test: $^*P \leq 0.05$). All experiments were repeated twice with similar results.

roles as signaling messengers in the immune system. A MAMP-induced ROS burst is often very fast and produced in the apoplast in Arabidopsis. The LPS-triggered first transient ROS burst is similar to that induced by other MAMPs. However, we found that LPS also triggered a second long-lasting ROS burst, which was largely associated with chloroplasts. In Arabidopsis, LORE was identified as an LPS sensor, which is required for the LPS-triggered first transient ROS burst. Surprisingly, we found that the LPS-triggered second ROS burst was still detectable in the *lore* mutants, indicating the presence of a redundant LPS recognition mechanism, in addition to LORE, which functions to trigger the second ROS burst.

MATERIALS AND METHODS

Plant Materials and Growth Conditions

All Arabidopsis (*Arabidopsis thaliana*) plants were Col-0 ecotype. Aequorin-expressing transgenic Arabidopsis was kindly provided by Marc Knight (Knight and Knight, 1995). *Lore* (Sail_857_E06) mutant seeds were obtained from the Arabidopsis Biological Resource Center (The Ohio State University). The seeds of other mutants, including *fls2-1* (Salk_026801), *bak1-4* (Salk_116202), *cerk1-2* (Gabi-Kat line, 096F09), and *lyk5-2* (Salk_131911), were previously described (Liang et al., 2013). For young seedling assays, Arabidopsis seeds were sterilized with 10% sodium hypochlorite, and then grown on half-strength Murashige and Skoog (MS) agar plates in a growth chamber (model A1000AR; Conviron) under a 16-h photoperiod at 22°C. For mature plant assays, plants were grown in pots containing Sunshine soil in a plant growth room under a 16-h photoperiod and 70% humidity at 22°C. Soybean (*Glycine max*), tomato (*Solanum lycopersicum*), *Nicotiana benthamiana*, rice (*Oryza sativa*), and barley (*Hordeum vulgare*) plants were grown in Sunshine soil in a plant growth room at 25°C with a 16-h photoperiod, and very young leaves were used for the ROS assay.

Chemical Reagents

All chemicals, unless otherwise mentioned, were purchased from Sigma-Aldrich. LPS (Sigma L9143) and flg22 (GenScript) were dissolved in sterilized ddH_2O.

Chemiluminescence Assay of ROS Production

ROS production was measured as described previously (Liang et al., 2013). In brief, leaf disks (0.2 cm^2) from dicot species or slices (0.2 $\times$ 0.5 cm) from monocot species were excised and incubated overnight in a 96-well plate with water. The following day, 200 μM luminol, 20 μg/mL horseradish peroxidase, and elicitors were added to each well. Isoluminol was used to detect the apoplastic ROS

burst since it is membrane impermeable. The chemiluminescent signal was immediately recorded using a Photek camera HRPCS5 (Photek).

Light Microscopy Observation of ROS Generation

DAB (3,3′-diaminobenzidine) staining was performed as previously described with some modifications (Liu et al., 2007). Healthy leaves were detached and placed in DAB solution (1 mg/mL, pH 3.5) for 12 h. The leaves were cleared by boiling in 95% ethanol for 10 min, chlorophyll was removed, and then the leaves were stored in 60% glycerol. The reddish-brown color of leaves was observed as H_2O_2 generation, and images were obtained under a light microscope (Nikon).

Confocal Microscopic Observation of ROS Generation

Intracellular H_2O_2 was measured using the membrane-permeable ROS indicator chloromethyl-2′,7′-dichlorodihydrofluorescein diacetate (CM-H2DCFDA; Invitrogen). CM-H2DCFDA staining and image acquisition were carried out as described previously with some modifications (de Torres Zabala et al., 2015). The chloromethyl group enhances the retention time of ROS within the cell. Two-week-old seedlings were treated with water, LPS (50 μg/mL), or flg22 (100 nM) for 1 h, and then CM-H2DCFDA (10 μM) was added 30 min before confocal observation followed by washing with distilled water for a few minutes. Fluorescence was analyzed under a confocal microscope using a 488-nm filter, with ROS signals being visualized at 501 to 556 nm and chlorophyll autofluorescence detected at 640 to 735 nm. Images were obtained under a confocal microscope (Zeiss). The GFP signal for transgenic plants expressing SSU-GFP was detected under the same conditions.

Aequorin Luminescence-Based Calcium Assay

A cytosolic calcium ($[Ca^{2+}]_{cyt}$) assay was performed as previously described with some modifications (Liang et al., 2013). Fifty microliters of water containing 10 μM coelenterazine (Nanolight Technology) was added per well in a 96-well plate. Vertically grown 5-d-old transgenic seedlings harboring the aequorin protein were individually transferred to each well and incubated overnight in the dark at room temperature. The following day, 50 μL of water containing the elicitor was added to each well, and the chemiluminescent signal was immediately recorded using a Photek camera HRPCS5. The remaining unchelated aequorin was discharged by adding 100 μL of 2 M $CaCl_2$ and 20% (v/v) ethanol. Photon counts were converted to calcium concentration.

Callose Deposition Assay

Arabidopsis seeds were germinated on half-strength MS agar plates and grown for 10 d, and then the seedlings were transferred to 24-well plates and treated with water, flg22 (100 nM), or LPS (50 μg/mL) for 24 h. Seedlings were fixed in ethanol and stained with 0.01% Aniline Blue (Clay et al., 2009). Images were obtained using a stereo microscope (Nikon) and callose was observed under UV excitation. The intensity was measured using Image J software.

RNA Isolation and RT-qPCR

Total RNA was extracted from 10-d-old seedlings using an RNeasy kit (Transgen) according to the manufacturer's instructions. First-strand cDNA was synthesized from 1 μg RNA using reverse transcriptase (Promega). A SYBR-Green master mix (Bio-Rad) was used for RT-qPCR reactions. RT-qPCR was performed using a Bio-Rad CFX60 real-time PCR device. After normalization to the *UBQ10* control, the relative levels of gene expression were calculated using the $2^{(-\Delta\Delta Ct)}$ method. All primers used for RT-qPCR are listed in Supplemental Table S1.

Immunoblotting Analysis

For protein immunoblotting, total protein was extracted using a buffer (50 mM pH 7.5 Tris-HCl, 150 mM NaCl, and 0.5% Triton X-100) containing protease inhibitors and the phosphatase inhibitor calyculin. Proteins were separated by 10% SDS-PAGE and transferred to polyvinylidene difluoride membranes (Bio-Rad) at 80 V for 2 h at 4°C. After blocking with 3% BSA, membranes were incubated with an antiphospho-p44/p42 MAP kinase antibody (Cell Signaling Technology). Signals were detected using Supersignal substrate (Pierce), and Ponceau S staining was used for loading control.

Bacterial Infection Assay

Five-week-old Arabidopsis leaves were infiltrated with water, flg22 (100 nM), or LPS (50 μg/mL) from the abaxial side. Twenty-four hours later, *Pseudomonas syringae* pv. *tomato* DC3000 (1×10^5 cfu/mL) was infiltrated into the same leaves. Seventy-two hours after bacterial inoculation, four leaf discs (1.5 cm^2) were ground in 500 μL of 10 mM $MgCl_2$ to extract bacteria, and serial dilutions were prepared for plating on NYG medium (5 g peptone, 3 g yeast extract, 2% glycerol, and 1.5% agar per liter) containing antibiotics.

VIGS Analysis

VIGS was performed as previously described (Liu et al., 2002). ROS was measured in the newly formed young leaves 20 d after infiltration.

Chlorophyll Fluorescence Imaging

Chlorophyll fluorescence imaging was performed as previously described with some modifications (de Torres Zabala et al., 2015). Arabidopsis wild-type seeds were germinated and grown on half-strength MS agar in a six-well plate for 2 weeks. Three seedlings were treated with water and another three were treated with LPS (50 μg/mL), and chlorophyll fluorescence imaging was performed using a CF Imager (FluorCam; Photon System Instruments). NPQ and maximum quantum yield (F_v/F_m) corresponding to PSII were calculated.

Isolation of LPS and Lipid A

LPS were extracted using the phenol-water method (Davis and Goldberg, 2012). Briefly, cultures of *P. syringae* DC3000 and *P. aeruginosa* PAO1 were harvested and mixed with equal volumes of buffer and phenol (~12.5 mg/mL) and left to stir at 68°C for 30 min. The samples were then centrifuged at 5,000*g* for 20 min, and the resulting aqueous layer was removed prior to adding further buffer to the phenol. The aqueous and phenol layers were then dialyzed against deionized water for 3 d in 1-kD MWCO dialysis bags. The dialyzed samples were then freeze dried. The lyophilized fractions were treated with RNase (50 μg/mL) and DNase (5 μg/mL) in 50 mM $MgCl_2$, pH 7.5, buffer overnight at 37°C. Proteinase K was then added to the samples, which were again digested overnight. The fully digested samples were then dialyzed as mentioned previously. The lyophilized fractions obtained from the aqueous layers were then dissolved in water and subjected to ultracentrifugation. The samples were centrifuged at 100,000*g* for 18 h at 4°C. The supernatants were removed and the LPS pellet was dried in the centrifuge tube. Lipid A was released by addition of 2% acetic acid at 100°C for 3 h and then separated by centrifugation at 3,000*g* for 10 min (Yi and Hackett, 2000). A small fraction of the purified LPS and lipid A was taken for SDS gel electrophoresis.

Accession Numbers

Sequence data from this article can be found in the GenBank/EMBL data libraries under the following accession numbers: *LORE* (At1g16380); *WRKY33* (At2g38470); *WRKY53* (At4g23810); *OXI1* (At3g25250); *VAR2* (At2g30950); *SSU* (At4g38460); *FLS2* (At5g46330); *BAK1* (At4g33430); *CERK1* (At3g21630); *LYK5* (At2g33580); and *PDS* (Solyc03g123760).

Supplemental Data

The following supplemental materials are available.

Supplemental Figure S1. LPS inhibit luminol activity.

Supplemental Figure S2. Count rate of the ROS burst trend over 24 h.

Supplemental Figure S3. MAP kinase phosphorylation over 24 h.

Supplemental Figure S4. Count rate of the ROS burst trend in different plant species.

Supplemental Figure S5. Comparison between isoluminol and luminol in the flg22-triggered rapid ROS burst.

Supplemental Figure S6. Detection of ROS in stomata and young cotyledons.

Supplemental Figure S7. Functional chloroplasts are essential for the lipopolysaccharides-triggered second ROS burst.

Supplemental Figure S8. Visualization of purified LPS and lipid A.

Supplemental Figure S9. A comparison of early accumulation of ROS in response to treatment with lipid A and flg22.

Supplemental Figure S10. LPS-triggered accumulation of ROS in known receptor mutants.

Supplemental Table S1. Sequences of the primers used in this study.

ACKNOWLEDGMENTS

We thank Dr. Gitta Coaker at UC Davis for kindly providing the plasmids for VIGS, Yaya Cui at the University of Missouri for providing the cultured cells of *P. syringae* DC3000 and *P. aeruginosa* PAO1, Dr. Shengyang He at Michigan State University for critical reading of the manuscript, and Dr. Jianbin Su and Dr. Xiaojian Xia at Zhejiang University for the suggestions regarding the photosynthesis assay.

Received November 15, 2017; accepted January 29, 2018; published February 5, 2018.

LITERATURE CITED

Adachi H, Nakano T, Miyagawa N, Ishihama N, Yoshioka M, Katou Y, Yaeno T, Shirasu K, Yoshioka H (2015) WRKY transcription factors phosphorylated by MAPK regulate a plant immune NADPH oxidase in *Nicotiana benthamiana.* Plant Cell **27:** 2645–2663

Antolín-Llovera M, Ried MK, Binder A, Parniske M (2012) Receptor kinase signaling pathways in plant-microbe interactions. Annu Rev Phytopathol **50:** 451–473

Asada K (2006) Production and scavenging of reactive oxygen species in chloroplasts and their functions. Plant Physiol **141:** 391–396

Baker CJ, Orlandi EW (1995) Active oxygen in plant pathogenesis. Annu Rev Phytopathol **33:** 299–321

Boller T, Felix G (2009) A renaissance of elicitors: perception of microbe-associated molecular patterns and danger signals by pattern-recognition receptors. Annu Rev Plant Biol **60:** 379–406

Braun SG, Meyer A, Holst O, Pühler A, Niehaus K (2005) Characterization of the *Xanthomonas campestris* pv. *campestris* lipopolysaccharide substructures essential for elicitation of an oxidative burst in tobacco cells. Mol Plant Microbe Interact **18:** 674–681

Camejo D, Guzmán-Cedeño Á, Moreno A (2016) Reactive oxygen species, essential molecules, during plant-pathogen interactions. Plant Physiol Biochem **103:** 10–23

Choi J, Tanaka K, Cao Y, Qi Y, Qiu J, Liang Y, Lee SY, Stacey G (2014) Identification of a plant receptor for extracellular ATP. Science **343:** 290–294

Clay NK, Adio AM, Denoux C, Jander G, Ausubel FM (2009) Glucosinolate metabolites required for an Arabidopsis innate immune response. Science **323:** 95–101

Daudi A, Cheng Z, O'Brien JA, Mammarella N, Khan S, Ausubel FM, Bolwell GP (2012) The apoplastic oxidative burst peroxidase in Arabidopsis is a major component of pattern-triggered immunity. Plant Cell **24:** 275–287

Davis MR Jr, Goldberg JB (2012) Purification and visualization of lipopolysaccharide from Gram-negative bacteria by hot aqueous-phenol extraction. J Vis Exp **63:** 3916

de Torres Zabala M, Littlejohn G, Jayaraman S, Studholme D, Bailey T, Lawson T, Tillich M, Licht D, Bölter B, Delfino L, et al (2015) Chloroplasts play a central role in plant defence and are targeted by pathogen effectors. Nat Plants **1:** 15074

Desaki Y, Kouzai Y, Ninomiya Y, Iwase R, Shimizu Y, Seko K, Molinaro A, Minami E, Shibuya N, Kaku H, et al (2018) OsCERK1 plays a crucial role in the lipopolysaccharide-induced immune response of rice. New Phytol **217:** 1042–1049

Galvez-Valdivieso G, Mullineaux PM (2010) The role of reactive oxygen species in signalling from chloroplasts to the nucleus. Physiol Plant **138:** 430–439

Gómez-Gómez L, Boller T (2000) FLS2: an LRR receptor-like kinase involved in the perception of the bacterial elicitor flagellin in Arabidopsis. Mol Cell **5:** 1003–1011

Hagar JA, Powell DA, Aachoui Y, Ernst RK, Miao EA (2013) Cytoplasmic LPS activates caspase-11: implications in TLR4-independent endotoxic shock. Science **341:** 1250–1253

Hörtensteiner S (2006) Chlorophyll degradation during senescence. Annu Rev Plant Biol **57:** 55–77

Jakubowski W and Bartosz G (2000). 2,7-Dichlorofluorescin oxidation and reactive oxygen species: What does it measure? Cell Biol Int **24:** 757–760

Jones JD, Dangl JL (2006) The plant immune system. Nature **444:** 323–329

Kadota Y, Sklenar J, Derbyshire P, Stransfeld L, Asai S, Ntoukakis V, Jones JD, Shirasu K, Menke F, Jones A, et al (2014) Direct regulation of the NADPH oxidase RBOHD by the PRR-associated kinase BIK1 during plant immunity. Mol Cell **54:** 43–55

King JD, Kocíncová D, Westman EL, Lam JS (2009) Review: lipopolysaccharide biosynthesis in *Pseudomonas aeruginosa*. Innate Immun **15:** 261–312

Knight H, Knight MR (1995) Recombinant aequorin methods for intracellular calcium measurement in plants. Methods Cell Biol **49:** 201–216

Lam JS, Taylor VL, Islam ST, Hao Y, Kocíncová D (2011) Genetic and functional diversity of *Pseudomonas aeruginosa* lipopolysaccharide. Front Microbiol **2:** 118

Lamb C, Dixon RA (1997) The oxidative burst in plant disease resistance. Annu Rev Plant Physiol Plant Mol Biol **48:** 251–275

Lambeth JD (2004) NOX enzymes and the biology of reactive oxygen. Nat Rev Immunol **4:** 181–189

Li L, Li M, Yu L, Zhou Z, Liang X, Liu Z, Cai G, Gao L, Zhang X, Wang Y, et al (2014) The FLS2-associated kinase BIK1 directly phosphorylates the NADPH oxidase RbohD to control plant immunity. Cell Host Microbe **15:** 329–338

Liang Y, Cao Y, Tanaka K, Thibivilliers S, Wan J, Choi J, Kang Ch, Qiu J, Stacey G (2013) Nonlegumes respond to rhizobial Nod factors by suppressing the innate immune response. Science **341:** 1384–1387

Liang Y, Tóth K, Cao Y, Tanaka K, Espinoza C, Stacey G (2014) Lipochitooligosaccharide recognition: an ancient story. New Phytol **204:** 289–296

Liu Y, Ren D, Pike S, Pallardy S, Gassmann W, Zhang S (2007) Chloroplast-generated reactive oxygen species are involved in hypersensitive response-like cell death mediated by a mitogen-activated protein kinase cascade. Plant J **51:** 941–954

Liu Y, Schiff M, Dinesh-Kumar SP (2002) Virus-induced gene silencing in tomato. Plant J **31:** 777–786

Lu YC, Yeh WC, Ohashi PS (2008) LPS/TLR4 signal transduction pathway. Cytokine **42:** 145–151

Macho AP, Zipfel C (2014) Plant PRRs and the activation of innate immune signaling. Mol Cell **54:** 263–272

Mahla RS, Reddy MC, Prasad DV, Kumar H (2013) Sweeten PAMPs: role of sugar complexed PAMPs in innate immunity and vaccine biology. Front Immunol **4:** 248

Martos GG, Terán MdelM, Díaz Ricci JC (2015) The defence elicitor AsES causes a rapid and transient membrane depolarization, a triphasic oxidative burst and the accumulation of nitric oxide. Plant Physiol Biochem **97:** 443–450

Maruta T, Noshi M, Tanouchi A, Tamoi M, Yabuta Y, Yoshimura K, Ishikawa T, Shigeoka S (2012) H_2O_2-triggered retrograde signaling from chloroplasts to nucleus plays specific role in response to stress. J Biol Chem **287:** 11717–11729

Mignolet-Spruyt L, Xu E, Idänheimo N, Hoeberichts FA, Mühlenbock P, Brosché M, Van Breusegem F, Kangasjärvi J (2016) Spreading the news: subcellular and organellar reactive oxygen species production and signalling. J Exp Bot **67:** 3831–3844

Mohamed KH, Daniel T, Aurélien D, El-Maarouf-Bouteau H, Rafik E, Arbelet-Bonnin D, Biligui B, Florence V, Mustapha EM, François B (2015) Deciphering the dual effect of lipopolysaccharides from plant pathogenic *Pectobacterium.* Plant Signal Behav **10:** e1000160

Nürnberger T, Brunner F, Kemmerling B, Piater L (2004) Innate immunity in plants and animals: striking similarities and obvious differences. Immunol Rev **198:** 249–266

O'Brien JA, Daudi A, Finch P, Butt VS, Whitelegge JP, Souda P, Ausubel FM, Bolwell GP (2012) A peroxidase-dependent apoplastic oxidative burst in cultured Arabidopsis cells functions in MAMP-elicited defense. Plant Physiol **158:** 2013–2027

Park J, Min JS, Kim B, Chae UB, Yun JW, Choi MS, Kong IK, Chang KT, Lee DS (2015) Mitochondrial ROS govern the LPS-induced pro-inflammatory response in microglia cells by regulating MAPK and NF-κB pathways. Neurosci Lett **584:** 191–196

Pinegin B, Vorobjeva N, Pashenkov M, Chernyak B (2018) The role of mitochondrial ROS in antibacterial immunity. J Cell Physiol

Qi J, Wang J, Gong Z, Zhou JM (2017) Apoplastic ROS signaling in plant immunity. Curr Opin Plant Biol **38:** 92–100

Ranf S, Gisch N, Schäffer M, Illig T, Westphal L, Knirel YA, Sánchez-Carballo PM, Zähringer U, Hückelhoven R, Lee J, et al (2015) A lectin S-domain receptor kinase mediates lipopolysaccharide sensing in *Arabidopsis thaliana*. Nat Immunol **16:** 426–433

Sena LA, Chandel NS (2012) Physiological roles of mitochondrial reactive oxygen species. Mol Cell **48:** 158–167

Shapiguzov A, Vainonen JP, Wrzaczek M, Kangasjärvi J (2012) ROS-talk - how the apoplast, the chloroplast, and the nucleus get the message through. Front Plant Sci **3:** 292

Silipo A, Molinaro A, Sturiale L, Dow JM, Erbs G, Lanzetta R, Newman MA, Parrilli M (2005) The elicitation of plant innate immunity by lipo-oligosaccharide of *Xanthomonas campestris*. J Biol Chem **280:** 33660–33668

Song DH, Lee JO (2012) Sensing of microbial molecular patterns by Toll-like receptors. Immunol Rev **250:** 216–229

Storek KM, Monack DM (2015) Bacterial recognition pathways that lead to inflammasome activation. Immunol Rev **265:** 112–129

Sun A, Nie S, Xing D (2012) Nitric oxide-mediated maintenance of redox homeostasis contributes to NPR1-dependent plant innate immunity triggered by lipopolysaccharides. Plant Physiol **160:** 1081–1096

Torres MA, Dangl JL, Jones JD (2002) Arabidopsis gp91phox homologues AtrbohD and AtrbohF are required for accumulation of reactive oxygen intermediates in the plant defense response. Proc Natl Acad Sci USA **99:** 517–522

West AP, Brodsky IE, Rahner C, Woo DK, Erdjument-Bromage H, Tempst P, Walsh MC, Choi Y, Shadel GS, Ghosh S (2011) TLR signalling augments macrophage bactericidal activity through mitochondrial ROS. Nature **472:** 476–480

Yang J, Zhao Y, Shao F (2015) Non-canonical activation of inflammatory caspases by cytosolic LPS in innate immunity. Curr Opin Immunol **32:** 78–83

Yi EC, Hackett M (2000) Rapid isolation method for lipopolysaccharide and lipid A from gram-negative bacteria. Analyst (Lond) **125:** 651–656

Zipfel C, Robatzek S, Navarro L, Oakeley EJ, Jones JD, Felix G, Boller T (2004) Bacterial disease resistance in Arabidopsis through flagellin perception. Nature **428:** 764–767

Zurbriggen MD, Carrillo N, Tognetti VB, Melzer M, Peisker M, Hause B, Hajirezaei MR (2009) Chloroplast-generated reactive oxygen species play a major role in localized cell death during the non-host interaction between tobacco and *Xanthomonas campestris* pv. *vesicatoria*. Plant J **60:** 962–973